IRANIAN JOURNAL OF CATALYSIS

Functionalized mesostructured silicas towards efficient conversion of furfuryl alcohol to ethyl levulinate

Rahul Prajapati[a], Sanjay Srivastava[a], Giriraj Jadeja[b], Jigisha Parikh[b]*

a) Department of Chemical Engineering, Government Engineering College, Valsad-396001, Gujarat, India

b) Department of Chemical Engineering, Sardar Vallabhbhai National Institute of Technology, Surat-395007, Gujarat, India

Received 6 April 2023; received in revised form 20 July 2023; accepted 7 August 2023 (**DOI: 10.30495/IJC.2023.1983480.2002**)

ABSTRACT

In this study, we synthesized ethyl levulinate (EL) by alcoholysis of furfuryl alcohol (FAL) with ethanol using two catalysts, SBA-15-SO_3H (SHS-15) and SBA-16-SO_3H (SHS-16). The catalysts were prepared through the hydrothermal method, and their physical and chemical properties were assessed using various techniques such as small and wide-angle XRD, N_2-sorption, SEM, TEM, FTIR, and Py-FTIR. Characterization results showed that SHS-15 possesses a mesoporous structure with a higher surface area and uniform pore size, along with moderate Brønsted acidity. In catalytic activity, both catalysts were tested for converting FAL to EL under moderate reaction conditions. SHS-15 exhibited excellent performance, achieving a yield of 93.9% for ethyl levulinate at 110°C, with a 0.5g catalyst dose, 1g FAL, and 4h reaction time. In contrast, SHS-16 yielded 88.6%, which was lower than SHS-15. These findings highlight the potential of SHS-15 as an effective catalyst for the alcoholysis of FAL into EL under moderate reaction conditions.

***Keywords**: Furfuryl alcohol, Ethyl levulinate, Ethyl alcohol, SHS-15, SHS-16*

1. Introduction

Now these days, most of the world's energy demands mainly depend on petroleum resources. However, owing to fluctuating petroleum prices, increasing living standards and therefore, progressively depleting these resources are becoming challenges to the world for securing energy needs [1]. According to the International Energy Agency (IEA) report (2021), approximately 84% of the world's energy demands were met through the consumption of conventional resources. And out of all conventional resources, almost 39.3 % (92.5 million barrels per day) of energy demand was fulfilled through crude oil where develop countries had almost 37% stacks and the rest for other world. In addition, dependency on petroleum & other fossil fuels is the major concern about global warming as well as environmental pollution. Petroleum emissions give rise to three main forms of pollution, namely air, water, and land. Each type of pollution can be attributed to distinct sources: air pollution is primarily caused by greenhouse gas emissions, water pollution results from oil spillage, and land pollution stems from activities associated with oil extraction. According to the Intergovernmental Panel on Climate Change (IPCC) 2019 report, approximately 34% of all anthropogenic (human-caused) greenhouse gas emissions were attributed to the energy sector, which includes emissions from the burning of petroleum products. To conquer the aforementioned issues of global energy security and to reduce environmental pollution, carbon-rich lignocellulosic biomass (LB) sources such as cellulose, hemicellulose, and lignin are looked upon as promising alternatives and are being widely used to convert it to transportation fuel & value-added chemicals [2]. One of the promising routes to convert cellulose and hemicellulose into transportation fuel & value-added chemicals is to produce 5-Hydroxymethylfurfural and furfural via triple dehydration of cellulose and hemicellulose-derived sugars. Thereafter, these furfural

*Corresponding author:
E-mail address: *jk_parikh@yahoo.co.in* (**J. Parikh**);

and 5-hydroxymethylfurfural are being used to produce various fuel additives and important industrial chemicals such as furfuryl alcohol, 2-methyl furan, levulinic acid, γ-valerolactone (GVL), 2, 5-dimethylfuran (DMF) and alkyl levulinates [3–6]. Among them, ethyl levulinate (EL) is known as an important chemical owing to a variety of applications such as it is used as an intermediate for the synthesis of fine chemicals, as a solvent in polymer industries, as a prime raw material for the synthesis of γ-valerolactone, and eventually, can be used as a fuel additive [3,7–9].

In general, EL can be synthesized from bio-based chemicals such as furfuryl alcohol (FAL) and levulinic acid (LA), through catalytic alcoholysis and esterification respectively [5,10–12]. Among both, however, FAL is widely used for the production of EL due to its easy availability at a low cost, fewer process steps [9,10,13,14], and most importantly the separation cost of EL from product mixture is less compared with LA as a raw material [2,3]. Conventionally, an alcoholysis of FAL was conducted in a homogeneous phase using protic acids such as HCl, ionic liquids, and H_2SO_4 [15–17]. Although EL yield could have been higher from biomass derivatives in homogeneously catalyzed reactions, significant challenges such as equipment corrosion, catalysts recycling, and environmental constraints are responsible for making it less attractive towards the production of EL [18,19]. Moreover, heterogeneous catalysts have been studied widely and reported to be promising alternatives due to their vast applicability as well as the capability to overcome the above-mentioned concerns [10,20].

In line with the above, a range of heterogeneous catalysts have been reported. Zhao et al. (2014) achieved 74.6 % EL yield from FAL using SO_4^{2-}/TiO_2 catalyst at 125 °C in 2 h [21]. Yogita et al. (2021) prepared β-zeolite supported by Zirconium-exchanged tungstophosphoric acid and at 130 ℃ reported 96% EL from FAL in 5 h [22]. Lange et al. (2009) studied semi-batch experiments for the synthesis of EL using FAL as a raw material over a range of catalysts such as sulfuric acid, zeolites, and ion-exchanged resins. Among all reported zeolites such as mordenite, H-Beta, ZSM-23, ZSM-12, ZSM-5, etc., maximum 65% EL reported at 125 ℃ and 7 $g_{fal}\ g_{cal}^{-1}\ h^{-1}$ feed rate over ZSM-5 (Si/Al=30) [23]. Nandiwale et al. (2015) also investigated zeolites such as H-ZSM-5, hierarchical zeolite, USY, and H-Beta for batch reaction, and an optimum yield of EL 73% was reported over hierarchical-HZ-5 zeolite at 140 ℃ in 4 h using FAL as a raw material [24]. However, Neves et al. (2014) reported an 80 % yield towards EL from FAL over mesostructured Al-TUD-1 catalyst at 140 °C in 24 h [25].

It is worth mentioning to note that the physical structure (surface area, pore size distribution, and morphology) of the catalysts and moderate acidity are the key factors that enable the yield of EL [10,26]. During the catalytic reaction, humus formation makes recovery hard, and low specific surface area limits the yield towards EL [27]. Like, a few carbon-based catalysts made from sugar or cellulose such as GC-PTSA-AC [28] and NC-FCM [29] have gained wide acceptance in acid-catalyzed reactions [30]. Song et al. (2015) reported an efficient conversion of levulinic acid (LA) and furfuryl alcohol (FAL) towards ethyl levulinate (EL) using hollow carbon spheres functionalized by arylsulfonic acid catalyst. They reported almost 85.9 % yield towards EL with FAL at 120 ℃ and 3 h over $ArSO_3H$-HMCSs***3.2***-1. At the same time 80% yield towards EL was reported when using LA as a raw material at 78 ℃ and 3 h over the same catalyst [31].

The mesoporous silica-based catalysts may be excellent materials with high surface area, strong thermal stability, and meso porosity. Prajapati et al. (2022) synthesized a silica-based composite mesoporous SBA-15/H-ZSM-5 catalyst and reported 89% yield towards EL from FAL at optimized reaction conditions of 110 °C in 5 h [26]. Whereas, Vaishnavi et al. (2021) prepared H-ZSM-5 catalysts with different SiO_2 to Al_2O_3 ratios (Si/Al) ranging from 5 to 160. These catalysts were then evaluated for their effectiveness in the alcoholysis of Furfuryl alcohol (FAL) to produce butyl levulinates (BL) and ethyl levulinate (EL). The results showed that the H-ZSM-5 catalyst with a Si/Al of 95 exhibited the highest BL selectivity of up to 85% under optimized conditions (temperature: 110 ℃, reaction time: 6 h). Conversely, when the same reaction conditions were applied, the maximum ethyl levulinate (EL) selectivity achieved over the H-ZSM-5 catalyst with a Si/Al of 95 was only 20% [2]. Chen et al. (2018) used Zr-SBA-15 as a catalyst for the production of methyl levulinate (ML) from furfural and reported a 36.5% yield at 270 ℃ in 10 h [32]. Furthermore, Li et al. (2020) used Zr-Al supported SBA-15 catalyst for the reaction of furfural to EL and reported a 67.2% EL yield at 180 ℃ in 3 h [33].

Brønsted acidity plays a crucial role in enabling the conversion of FAL to EL through the process of alcoholysis. Liu et al. (2016) observed that the density of Brønsted acidic sites has a considerable impact on the catalytic activity. Specifically, a higher Brønsted acidity led to increased yields of EL through FAL alcoholysis [27]. Furthermore, Zhao et al. (2019) accomplished a

67.1% ethyl levulinate (EL) yield from furfuryl alcohol (FAL) at 150 ℃ in 1 h using a sulfonated glucose-derived catalyst. The presence of the -SO_3H-C catalyst enhanced Brønsted acidity and catalyst activity, leading to a 57.3% EL yield even after being used for four cycles [34]. In a separate study, Yang et al. (2019) developed a GC-PTSA-AC catalyst through mono-functional hydrothermal carbonization of glucose, functionalized with acrylic acid and p-toluenesulfonic acid. This catalyst was tested for the alcoholysis of FAL to produce butyl levulinate (BL), yielding an excellent 91% BL yield at 120 ℃ in 4 h. The -SO_3H group and the -COOH group in the catalyst exhibited strong synergy, resulting in an almost 89% BL yield even after the fourth cycle [28]. Additionally, for further exploration of carbonaceous solid acid catalysts, Yu et al. (2020) synthesized a carbon-based catalyst from sulfite pulping industry pulp using a direct sulfonating lignosulfonate method with -SO_3H and -COOH functional groups. This catalyst displayed excellent performance towards the conversion of FAL to butyl levulinate, yielding 95% at 110 ℃ in 8 h [35]. Meanwhile, H. Guo et al. (2020) employed a one-pot carbonization method using 5-sulfosalicylic acid and ammonium formate to prepare NC-FCM catalyst from cellulose. They investigated the alcoholysis of FAL and levulinic acid (LA) to produce EL. The catalyst achieved an approximate 65% EL yield from FAL at 150 ℃ in 6 h and a 90% EL yield from LA at 120 ℃ in 8 h [29].

In this study, the focus was to improve the yield of EL (ethyl levulinate) through FAL (furfuryl alcohol) alcoholysis. To achieve this, the structure and acidity of silica-based catalysts, namely SBA-15 and SBA-16, were modified by treating them with sulfonic acid salt. The catalysts, after tuning, were denoted as functionalized mesoporous SHS-15 and SHS-16 materials. These newly prepared catalysts were then utilized for the conversion of FAL to EL at moderate reaction conditions. Additionally, the impact of reaction parameters, including temperature, catalyst dosage, reaction time, and FAL to ethanol ratio (w/w), on the maximum yield of EL was investigated using the screened catalyst.

2. Experimental

2.1 Materials

Pluronic-123 (P-123: $PEO_{20}PPO_{70}PEO_{20}$), Pluronic F-127 (F-127: $PEO_{106}PPO_{70}PEO_{106}$), tetraethylorthosilicate ($Si(OC_2H_5)_4$) (TEOS) having a purity of 95%, (3-Mercaptopropyl) trimethoxysilane (MPTMS: $HS(CH_2)_3Si(OCH_3)_3$), furfuryl Alcohol ($C_5H_6O_2$) (FAL) and ethyl levulinate ($C_7H_{12}O_3$) (EL) were purchased from Sigma Aldrich, Mumbai, India, wherein, both FAL and EL were having a purity of 99%. An analytical grade (AR) materials hydrogen peroxide (H_2O_2) solution (30%, v/v), hydrochloric acid (HCl) (37%), 98% purified sodium hydroxide (NaOH) pallets, 98% purified N-butanol ($C_4H_{10}O$) and 99.9 % purified ethyl alcohol (C_2H_5O), were procured from LABORT Fine Chem Pvt. Ltd., India.

2.2 Catalysts Preparation and Characterization

2.2.1 Preparation of SBA-15-SO_3H (SHS-15) catalyst

SBA-15 (S-15) was synthesized following the procedure reported by Zhao et al. (2010) [36]. In a unique approach, 4 g of P-123 was dissolved in an acid solution containing 184 mL of deionized water and 23.4 mL of 37% HCl and kept on continuous stirring at 400 rpm for 3 h at a temperature of 303 K in a polypropylene bottle. Subsequently, 12.70 g of TEOS was added to the above solution, and the temperature was raised to 313 K. The solution was further mixed at 400 rpm for 24 h. Thereafter, the solution was transferred in a hot air oven at 373 K for an additional 24 h. The resulting filtered cake was washed with distilled water until it reached a neutral pH. Following this, the cake was dried overnight at 353 K. To obtain the final powdered form of S-15, the dried cake was calcined at 823 K for 6 h.

SHS-15 was synthesized following the methodology reported by Zhou et al., (2014) and Shah et al., (2014) [37,38]. In this distinct procedure, 4 g of P-123 was dissolved with constant stirring (400 rpm) in an acid solution composed of 184 mL of deionized water and 23.4 mL of 37% HCl. The dissolution process took place for 3 h at 303 K inside a polypropylene bottle. After that, 12.70 g of TEOS was added and allowed to pre-hydrolyze for at least 30 min. Following this, the MPTMS-H_2O_2 solution was added. The resulting mixture was continuously stirred (400 rpm) for 24 h at 313 K. Subsequently, a tightly-capped polypropylene bottle containing the solution was kept in an oven at 373 K for 24 h. The resulting precipitate was filtered and washed with deionized water to achieve a neutral pH. The obtained cake was then dried overnight at 353 K and continuously refluxed for 24 h using 350 mL of ethanol as the solvent for every 1.5 g of the product. Finally, the resulting product was washed with ethanol and dried at 373 K for 6 h to obtain the desired functionalized mesoporous silica with larger pores.

2.2.2 Preparation of SBA-16-SO3H (SHS-16) catalyst

SBA-16 (S-16) catalyst was synthesized by following the procedure of dos Santos et al. (2013) [39]. In a distinct procedure, a tightly-capped polypropylene bottle containing 120 mL of 2 M HCl solution was prepared at room temperature. To this, 2 g of F-127 was added, and the mixture was continuously stirred at 400 rpm. After 2 h, 8.3 g of TEOS was introduced, followed by the addition of 6 g of N-Butanol as a co-surfactant. The sol-gel mixture was stirred continuously at 400 rpm for 24 h at 313 K. The resulting aqueous gel underwent a pre-treatment process in an air oven at 373 K for 24 h. The product was then filtered using distilled water until a neutral pH was reached. Subsequently, it was dried overnight at 353 K and calcined at 823 K for 6 h to obtain the final powder form of the S-16 catalyst.

SBA-16–SO_3H synthesis was conducted following the methods outlined by Zhou et al., (2014), dos Santos et al., (2013), and Chaudhuri et al., (2017) [37,39,40]. The procedure involved dissolving 2 g of F-127 in 120 mL of 2 M HCl within a tightly-capped polypropylene bottle at 308 K, with constant mixing at 400 rpm. After 2 h, 8.3 g of TEOS and 6 mL of N-Butanol were added dropwise, and the mixture was allowed to pre-hydrolyze for approximately 45 min. Next, the MPTMS-H_2O_2 solution was introduced and stirred for 24 h at 313 K. Subsequently, the formed gel was transferred to an air-tight-capped polypropylene bottle and placed in a hot air oven at 373 K for another 24 h. Subsequently, the white gel was filtered using deionized water until it reached pH neutrality. The obtained product was dried overnight in an air oven at 353 K and then refluxed in ethanol (350 mL/1.5 g) for 24 h. The final product (SHS-16 catalyst) was washed with ethanol at room temperature and dried at 373 K for 6 h.

2.3 Catalyst characterization

The properties of various prepared catalysts were evaluated using small & wide-angle X-ray diffraction (XRD), Transmission electron microscopy (TEM), Scanning electron microscopy (SEM), and Nitrogen adsorption-desorption (BET) [26], Acid-base titration [41], Fourier Transform Infrared spectroscopy (FTIR) and Pyridine-Fourier Transform Infrared spectroscopy (Py-FTIR) as reported elsewhere [37].

2.4 Catalytic activities

All reactions took place in a 100 mL autoclave reactor acquired from Amar Equipment Pvt. Ltd, Mumbai (refer to **Fig. 1**). In summary, the procedure involved adding 1 g of FAL to a reactor containing 20 mL of ethanol and 0.5 g of the catalyst. Catalyst screening involved conducting reactions at 110 ºC, 10 bar nitrogen pressure at 800 rpm. The product mixture was analyzed using Gas Chromatography (GC) with an FID detector, by Sigma Instrument Pvt. Ltd., Vadodara.

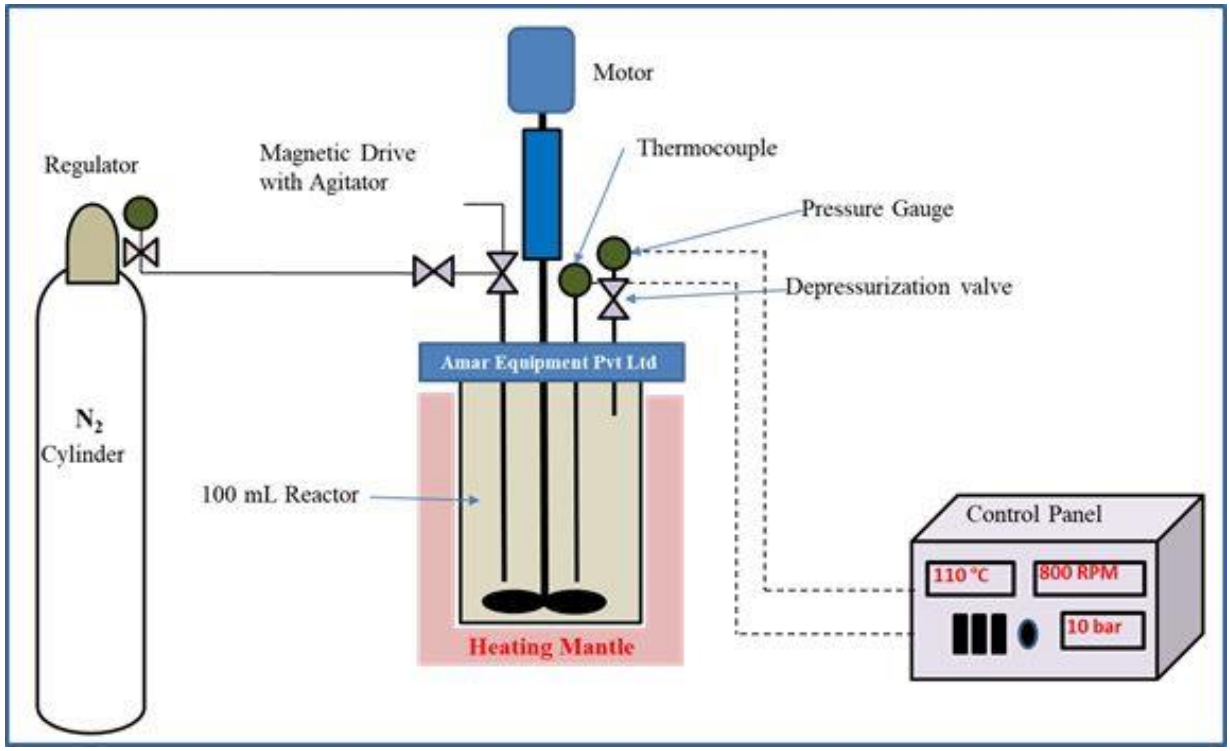

Fig. 1 Schematic diagram of reaction set-up

3. Results and Discussion

3.1 Catalyst Characterization

3.1.1 X-ray diffraction

All the prepared catalysts were analyzed using small angle XRD in the 2θ range of 1° to 5° in order to see their meso structure indexing as depicted in **Fig. 2**. It can be easily seen that catalysts S-15 & SHS-15 showed notable small-angle reflection at 2θ equal to 1°, 1.6°, and 1.8° corresponding to (100), (110) and (200), respectively. Similarly, S-16 & SHS-16 also showed notable small-angle reflection at 2θ equal to 1°, 1.6°, and 1.8° corresponding to (110), (200) and (211), respectively. These diffraction patterns are indicating the presence of 3D cubic structures in all the synthesized mesoporous materials and all could have highly ordered 2D hexagonal structures which are in collaboration with the following TEM results [37,38,40,42].

However, a slight decline of peak intensity with little shift in a peak position to a higher angle in sulfonated materials might be indicating the presence of –SO_3H due to the decrease in the d-spacing of S-15 & S-16 materials. **Fig. 3** depicts the wide-angle XRD spectra of all the prepared catalysts. The broad peak at a 2θ angle between ~ 22° to 30° attributes an amorphous silica structure in both S-15 & S-16 [39]. However, after treatment with sulfonic acid, both SHS-15 & SHS-16 showed slightly intense peaks between the same 2θ angles which might be ascribed to the enhanced crystalline structure of both the materials.

3.1.2 BET Analysis

To analyze the various textural properties such as BET surface area, pore volume, and pore size of various prepared catalysts, all four samples were characterized using N_2-sorption analysis (see **Table 1** & **Fig. 4**). In accordance with IUPAC nomenclature, all four catalysts showed type IV hysteresis isotherms (see **Fig. 4a**) [37,39,42], wherein, both S-15 and SHS-15 displayed Type H1 hysteresis loops, attributing the presence of uniform sizes and shapes [37,38]. However, S-16 and corresponding SO_3H-modified SHS-16 displayed the type H4 hysteresis loops which might correspond to fewer amounts of mesopores that may be restricted by micropores. In addition, the hysteresis loop for SO_3H-modified S-15 is at relatively high pressures around 0.8–1.0 to SO_3H-modified S-16 which confirms the retention of the mesoporous structure of S-15 even after SO_3H modification. **Fig. 4b** depicts bimodal pore size distributions of SHS-15 & SHS-16 having an average pore size of ~14.5 nm & ~4.5 nm indicating confine mesopores.

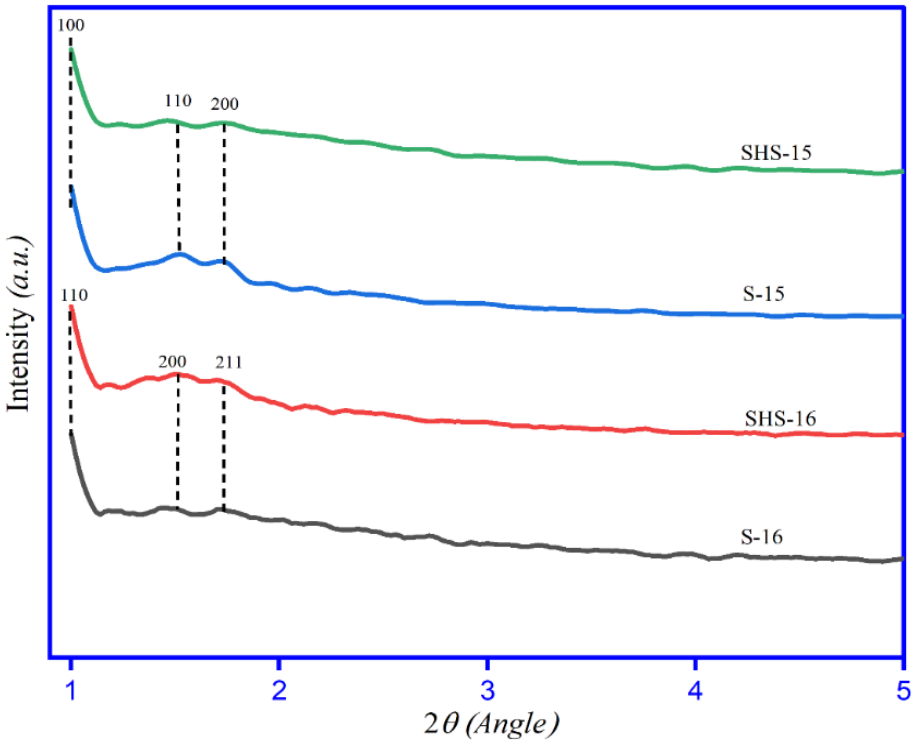

Fig. 2 Small angle XRD patterns for solid acid catalysts

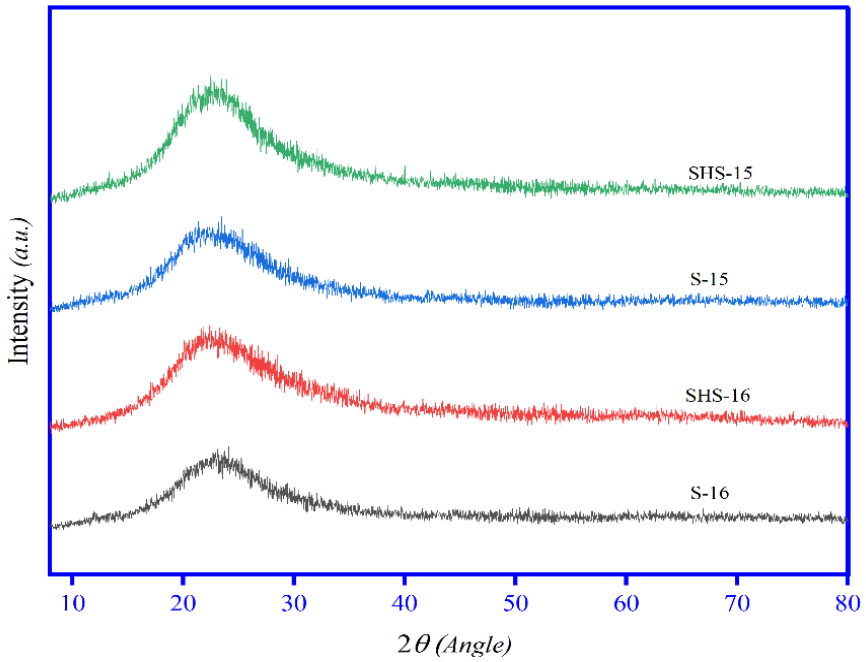

Fig. 3 Wide angle XRD patterns for solid acid catalysts

Table 1 Textural properties of all catalysts

Samples	S_{BET} (m^2/g)	Pore Volume(cm^3/g)	Pore -Dp (nm)	Total Acidity* (mmol/gCat)
S-15	508.11	0.780	3.05	0.01
S-16	596.21	0.317	3.41	0.03
SHS-15	587.17	0.882	3.83	1.30
SHS-16	582.62	0.458	3.06	1.08

*Using the NaOH titration method [41]

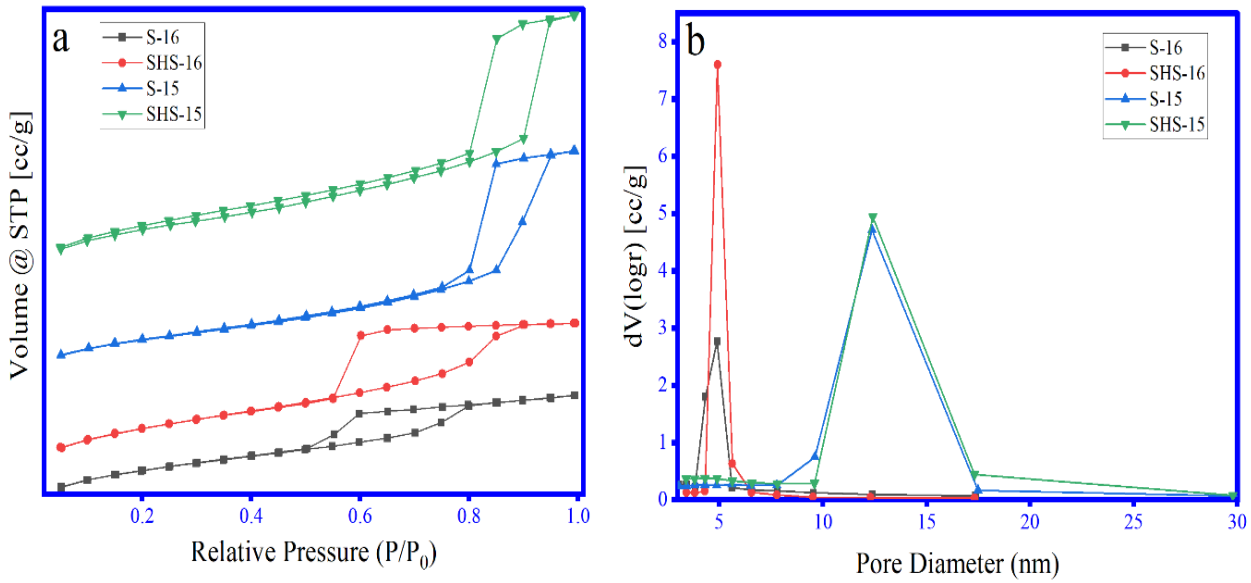

Fig. 4 The N_2 adsorption-desorption isotherms of solid acid catalysts& their pore distribution

3.1.3 Acidity measurement via NaOH titration method

The total acidic sites of prepared catalysts were evaluated via titration method (Acid-Base) with sodium hydroxide (NaOH) as an ion-exchange agent [41]. Concisely, at room temperature 0.1 g catalyst was placed in 60 mL of 0.008 M NaOH solution under stirring at 250 rpm for 30 mins followed by titration against 0.02 M HCl with phenolphthalein as an indicator. The total acidity was calculated as per Eq.1. The results are presented in **Table 1**.

$$\text{Total acidity } (\text{mmol} g_{cat}^{-1}) = \frac{(V_{NaOH}M_{NaOH} - V_{HCL}M_{HCL})}{W_{catalyst}} \times 1000 \quad \text{(Eq.1)}$$

where V is Volume (L), M is molarity (gmol/L) and W represents catalyst weight (g).

It is to be noticed that both mesoporous silicas S-15 & S-16 are known to be neutral support materials and hardly showed any surface acidity. However, after the incorporation of the -SO_3H group in both S-15 & S-16 the amount of acidity was increased (see **Table 1**). Further, the strength of Lewis and Brønsted acidic sites will be confirmed via Py-FTIR.

3.1.4 Py-FTIR

To get insights into the nature of acidity (Lewis and Brønsted), both SHS-15 & SHS-16 were analyzed with Pyridine-FTIR (see **Fig. 5**). It can be deduced that both the catalysts showed the vibration at 1450 cm^{-1}, 1490 cm^{-1} and 1546 cm^{-1}, wherein, vibrations at 1450 $cm^{-1}$and 1490 cm^{-1} confirms the existence of the Lewis acid sites and combined Lewis and Brønsted acidity [37]. The occurrence of Lewis acidity may be attributed to the interaction of –SO_3H to mesoporous silica framework with Pyridine. However, the presence of reasonable Brønsted acidity at 1546 cm^{-1} might be attributed to structured effects via ≡Si-OH stretching which is further confirmed by FTIR analysis [37,42]. It is believed that the interaction of sulfonic -SO_3H to the silica framework enhances both (L+B) acidic sites in SHS-15 & SHS-16 materials and therefore, get better accessibility to the furfuryl alcohol and ethanol to react on said acidic sites [37,42].

3.1.5 Scanning Electron Microscopy Analysis

Scanning Electron Microcopy was used to analyze the morphology and the structure of prepared S-15 and corresponding -SO_3H modified samples (see **Fig.6a** & **6b**). According to the findings presented in Fig. 6a, the S-15 samples exhibited a wire-like shape with a relatively uniform size. The uniformity in size suggests that the synthesis method used for preparing the S-15 samples was successful in producing homogeneous structures. This observation is consistent with previously reported results in the literature [37]. On the other hand, **Fig.6b** reveals a distinct morphology for the SHS-15 sample. Instead of individual wire-like structures, the SHS-15 samples appear as aggregates or clusters of structures. This observation suggests that the modification with -SO_3H groups has influenced the self-assembly behavior of the S-15 material, leading to the formation of aggregated structures. The aggregation might be attributed to the introduction of new functional groups, which could promote intermolecular interactions and the formation of larger assemblies [36,38,39]. These findings provide valuable insights into the effect of -SO_3H modification on the morphology and self-assembly behavior of the material.

3.1.6 Transmission Electron Microscopy

To confirm the hexagonal structure of S-15 and the confinement of -SO_3H within its framework, both S-15 and SHS-15 materials were characterized further via TEM analysis and displayed in **Fig. 7**. In S-15 **Fig.7a**, dark walls with white channels are clearly observed, whereas in **Fig.7b**, due to –SO_3H integration the amorphous arrangement has been formed over S-15 regular mesoporous structure which is visible via shadowy. It is also noticed that there was no major structural change has been found, revealing the catalyst structure remains intact [36,38].

3.1.7 Fourier Transform Infrared Spectroscopy

FTIR was carried out for all four samples namely S-15, SHS-15, S-16, and SHS-16 to get more insight into the functional groups present and to observe structural changes via -SO_3H modification over the S-15 & S-16 samples, and the results are presented in **Fig. 8**. The O-H stretching vibration at 3445 cm^{-1} corresponds to the presence of surface hydroxyl groups in all the prepared samples. The peaks at 1080 cm^{-1} and 794 cm^{-1} can be ascribed to asymmetric & symmetric stretching of Si–O–Si, correspondingly. In addition, SO_3H-modified samples showed a vibration of just 1643 cm^{-1}, which might be attributed to O-H deformation [37,42].

3.2 Catalytic Activity

Alcoholysis of FAL towards EL was carried out over mesoporous silicas S-15, S-16, and their -SO_3H modified versions such as SHS-15 and SHS-16. The results are presented in **Table 2**, wherein, it can be

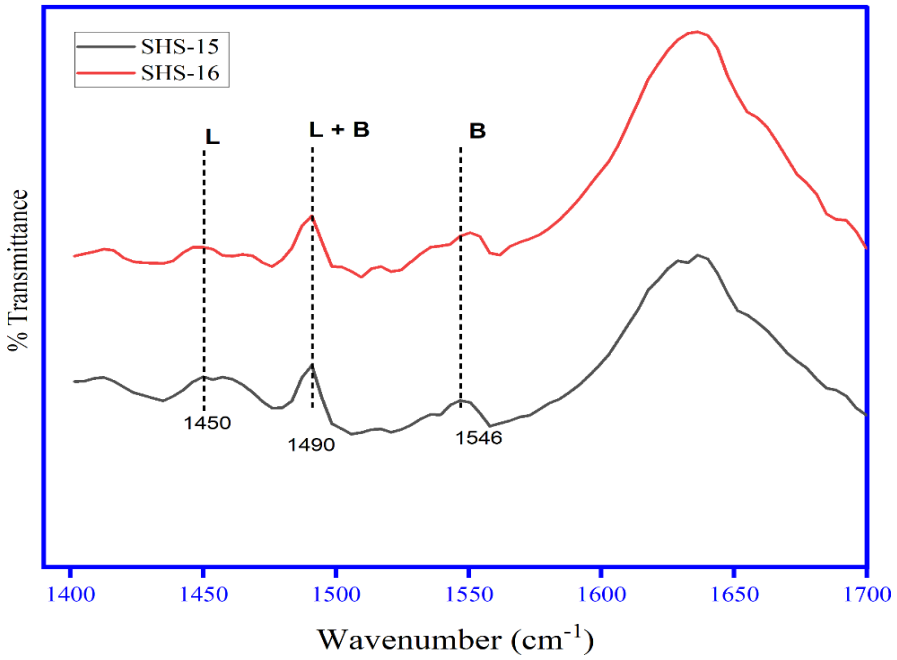

Fig. 5 Py-FTIR spectra of SHS-15 and SHS-16.

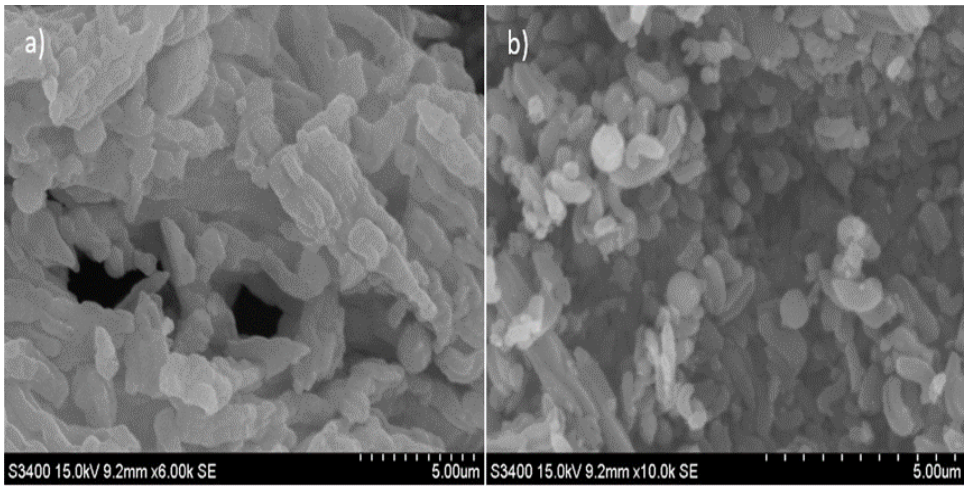

Fig. 6 SEM images (a) S-15 (b) SHS-15

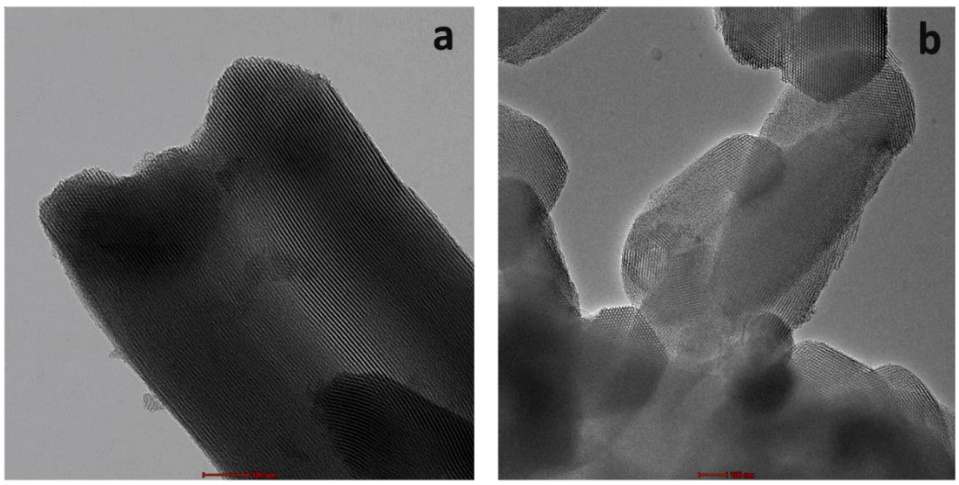

Fig. 7 TEM images (a) S-15 and (b) SHS-15

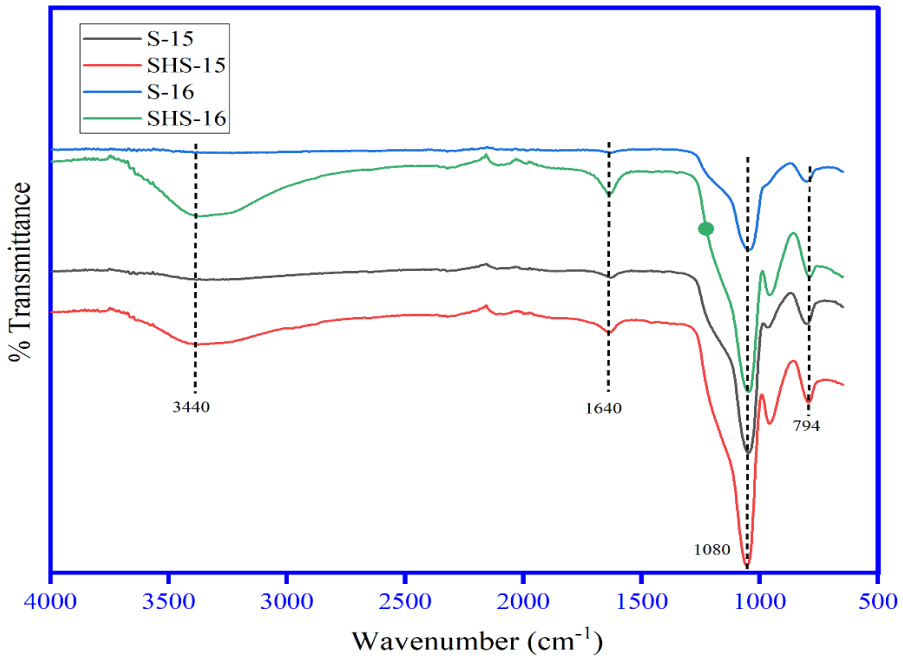

Fig. 8 FT-IR spectra of S-15, SHS-15, S-16, and SHS-16

observed that both mesoporous silicas S-15 and S-16 showed very low conversion of FAL.Less than two percent EL was formed over both these mesoporous silicas. When looking into the various characterization results, it could be easily understood that since both the catalysts didn't have much acidity which is a key aspect for the conversion of FAL to EL and therefore, resulted in low conversion. However, DEE formation on these two materials is mainly attributed to the shape-selective nature of these support materials wherein, mesoporosity of both S-15 & S-16 favors the formation of DEE by etherification of FAL to EL [5,21,43]. In contrast to this, both -SO_3H modified versions such as SHS-15 and SHS-16 have shown almost 100% and 89.6% conversion, respectively, with 88.6 % yield with SHS-16 and > 93% yield with SHS-15. The higher conversion of FAL and yield towards EL in both SHS-15and SHS-16 catalysts can be explained by taking into consideration the various characterization data, in which, results principally corroborated to the total number of (L+B) acidic sites, mesoporous structure of both the catalysts. The combination of both acidity and shape-selective nature of both the catalysts results in better yield towards EL. However, when compared with SHS-16, a drastic increase in the conversion of FAL (11% more) and EL yield (5% more) over SHS-15 may be attributed to the uniform hexagonal structure and increased total acidity of the said catalyst. It is to be noticed that SHS-16 has shown an H4 hysteresis loop and hence has fewer mesopores in it. Siva Sankar et al. (2017) reported similar results over a TPA-doped S-16 catalyst for the conversion of FAL towards BL [44].

Table 2 Catalyst Activity for the conversion of FAL to EL

Catalyst	Temp. ℃	Time (h)	% Conversion	% Y_{EL}	Ref.
S-15[a]	110	4	12.12	1.62	Present study
S-16 [a]	110	4	10.84	2.43	Present study
SHS-15 [a]	110	4	100	93.94	Present study
SHS-16 [a]	110	4	89.62	88.66	Present study
NB-H-ZSM-5	120	6	100	64.7	[1]
SBA-15/H-ZSM-5	110	5	100	89	[26]
$ArSO_3H$-HMCSs*3.2*-1	120	3	100	85.9	[31]
Mesoporous MIL101(Cr)-SO_3H	160	2	100	83.8	[45]
Mesoporous SO_4^{2-}/Al_2O_3	200	3	100	80.6	[46]

[a] Conditions: (0.5 g catalyst, 1 g reactant (FAL) in 20 mL Ethanol, rpm 600 and N_2 Pressure 10 bar)

The catalytic activity and selectivity of the present catalytic system were compared with recent literature published on the conversion of FAL to EL (ref. **Table 2**, Entry 5-9). Prajapati et al. (2022) revealed the role of the shape-selective nature of catalyst wherein, a mesoporous SBA-15/HZSM-5 catalyst exhibited almost 89% yield towards EL [26]. Zhang et al. (2019) synthesized mesoporous sulfate-based alumina catalyst which shows almost 81% EL yield. Whereas, Song et al. (2015) demonstrated the role of Brønsted acid sites by attaching arylsulfonic acid to a hollow mesoporous carbon sphere and reported 85.9% EL yield [31]. Li et al. (2022) reported almost 65% EL yield through FAL over Nano-H-SZM-5 zeolite [1]. However, Liu et al. (2019) incorporate Brønsted acidity into Metal-Organic Framework (101) using a sulfonated ($–SO_3H$) group and reported almost 84% EL yield. Eventually, SHS-15 which is reported in the present study was found to be a superior catalyst in terms of yield towards EL amongst given in **Table 1**.

3.3 Effects of Parameters Studied

3.3.1 Effect of Temperature

The impact of reaction temperature on the conversion of FAL to EL was investigated within the range of 80 °C to 120 °C (refer to **Fig. 9**). It was noticed that as the temperature rose from 80°C to 110°C, the conversion of FAL significantly increased from 25% to nearly 100%. However, no substantial changes were observed when the temperature was further raised to 120 °C.

As far as yield towards EL is concerned, similar increasing trends (10% to 93.9%) were observed between 80 °C to 110 °C. However, a again increase in temperature from 110 °C to 120 °C, leads to a decrease in yield towards EL owing to unknown by-product formation [45,47]. Moreover, at below 80 °C and above 110 °C, side reactions might become more favorable, resulting in the formation of by-products. At low temperatures, as the solubility of reactants and products may change, influencing the progress of the reaction and potentially leading to the formation of unforeseen by-products. In addition, low temperatures can lead to changes in the orientation and accessibility of reactive sites on molecules, affecting the selectivity of the reaction and promoting the formation of by-products [5,45]. However, when the reaction temperature increases, the intermediate converts to the targeted product EL rather than other products. This suggested that the conversion of intermediates depends on the reaction temperature and these results are in argument with that in literature [26,32,44].

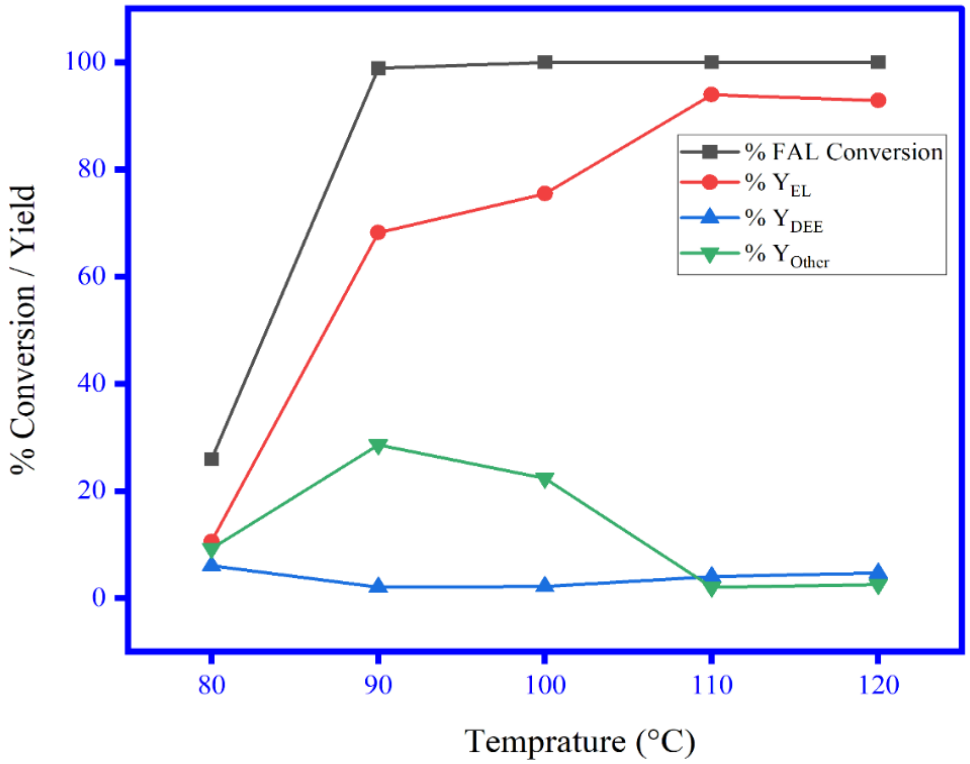

Fig. 9 Effect of Temperature (Reaction conditions: 0.5 g catalyst, 1 g reactant (FAL) in 20 mL Ethanol, time 4 h, rpm 600 and N_2 Pressure 10 bar)

3.3.2 Effect of Catalyst Amount

The available number of active sites plays an important role in the alcoholysis reactions. Herein; a variation of the catalyst amount from 0.2 g to 0.6 g and looked at the conversion of FAL towards the EL (see **Fig. 10**). As per **Fig. 10**, with increases in catalyst amount, the yield towards EL is increased, however, the total yield towards DEE and by-products decreases.

The main reason for these trends is the available number of active sites of catalysts which increased with the increasing amount for the same. The more active sites available to the intermediate product led to an increase in 93.9 % EL yield towards EL at 0.5 g catalysts dose. The observations are well-matched with the literature published [18,44]. It was also noticed that further catalyst dose increased from 0.5 g to 0.6 g, and there was very less changed observed in the EL yield.

3.3.3 Effect of Furfuryl Alcohol

FAL concentration [(1 g to 1.75 g FAL) in fixed 20 mL ethanol] was studied to see the trend in EL formation which is presented in **Fig. 11**, over the SHS-15 catalyst. As observed when FAL concentration increases, both the conversion of FAL and yield towards EL decreased and the highest conversion of FAL (100%) and corresponding yield towards EL (93.9%) was observed at 1 g FAL in 20 mL of EtOH.

As the active surface area in the reaction mixture is constant, the declining trend may be attributed to the less active sites available for the conversion of FAL when the concentration of FAL increased. Therefore, a dilute concentration of FAL is essential to carry out the said reaction with ethanol as solvent [26,44].

3.3.4 Effect of Reaction Time

Reaction time is an important parameter to study from an economical point of view as lesser time may conserve energy and may ultimately reduce the cost of the product [44,48]. In this context, the conversion of FAL to EL is carried out by varying the time from 2 h to 5 h using SHS-15 catalyst with all other parameters intact (ref. **Fig. 12**). As observed, the conversion of FAL was low (46%) in two hours, however when the reaction proceeded to 3 h, conversion reached to 80%. After 4 h, the conversion reaches 100% and it remained the same for 5 h.

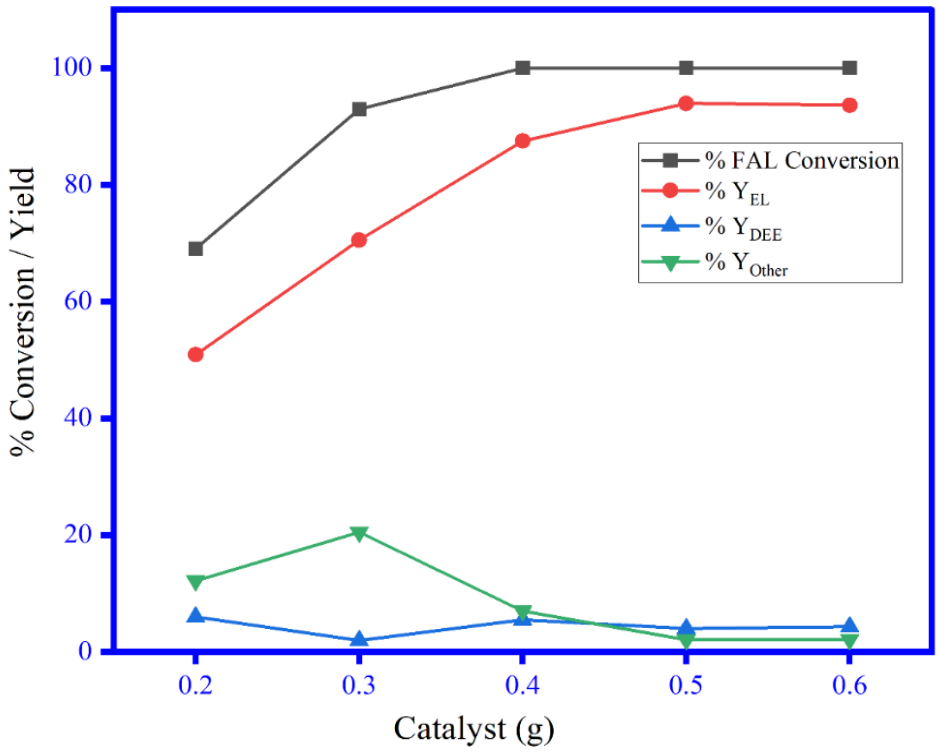

Fig. 10 Effect of Catalyst amount (Reaction conditions: Temperature 110 ˚C, 1 g reactant (FAL) in 20 mL Ethanol, time4 h, rpm 600 and N_2 Pressure 10 bar)

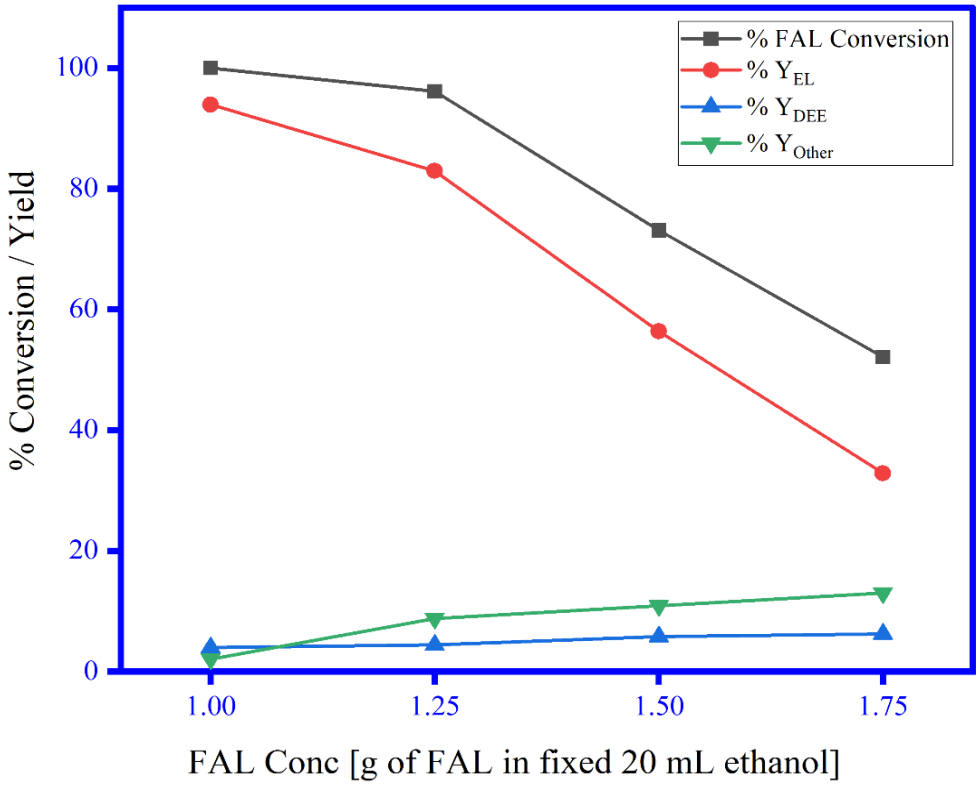

Fig. 11 Effect of Reactant (FAL) concentration (Reaction conditions: Temperature 110 ˚C, 0.5 g catalyst, and rpm 600 and N_2 Pressure 10 bar)

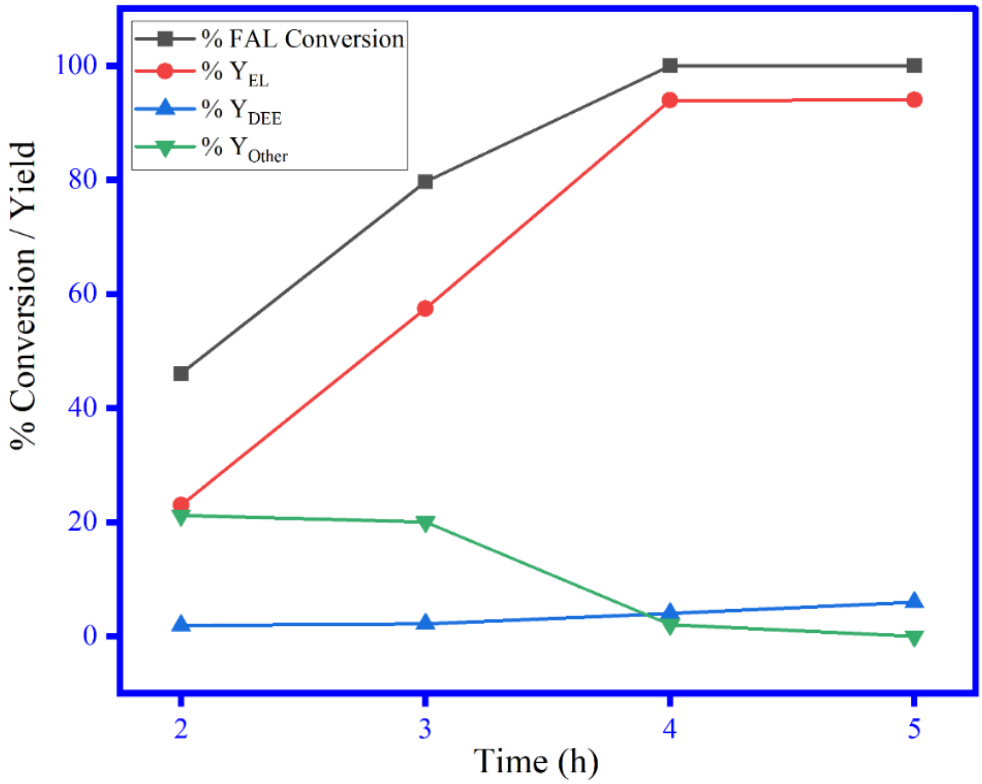

Fig. 12 Effect of Reaction time (Reaction conditions: Temperature 110 ˚C, 1 g reactant (FAL) in 20 mL Ethanol, 0.5 g catalyst, and rpm 600 and N_2 Pressure 10 bar)

As far as yield towards EL is concerned, it increased from 2 h to 4 h (23% to 93.9%), however, no significant changes were observed when the reaction was continued further to 5 h. These observations exhibit the fast conversion of FAL to the intermediate ethoxymethylfuran and further its transformation towards EL and reducing the conversion of other products which might be the rate-limiting step. The observations are in accordance with results published in the literature [45,49]. Moreover, these results provide valuable insights into the kinetics of the reaction and highlight the importance of optimizing the reaction time for maximizing the yield of the desired product.

4. Conclusions

In conclusion, both S-15 and S-16 showed very less conversion as well as yield towards EL owing to having negligible acidic strength. However, functionalized mesostructured silicas i.e. SHS-15 and SHS-16 have shown almost 100% and 89.6% conversion, respectively, with 88.6% yield with SHS-16 and >93% yield with SHS-15, at temperature 110 ˚C in 4 h. The higher conversion and yield towards EL over functionalized mesostructured silicas i.e. SHS-15 and SHS-16 could be attributed to the appropriate combination of surface structure and surface acidity as evidenced from XRD, BET, TEM, and Py-FTIR results. In addition, the more yield towards EL on SHS-15 corresponds to the more hexagonal porous arrangement in comparison to the SHS-16 as evidenced through BET & TEM results. The effect of parameters revealed that by increasing the temperature, the conversion of FAL increases with an enhanced yield towards EL. Similarly, time also had a major impact on the yield towards EL as prolonged time resulted in more conversion of intermediate towards EL. However, when the amount of catalyst increases, the conversion of FAL increased as more active sites were available for the reaction. Eventually, FAL concentration had negative effects on the yield.

Acknowledgements

We gratefully acknowledge Shree Dhanvantary Pharmacy College, Kim for FTIR and SICART, Anand for TEM analysis.

References

[1] Y. Li, S. Wang, S. Fan, B. Ali, X. Lan, T. Wang, ACS Sustain. Chem. Eng. 10 (2022) 3808–3816.

[2] B.J. Vaishnavi, S. Sujith, N. Kulal, P. Manjunathan, G.V. Shanbhag, Mol. Catal. 502 (2021) 111361.

[3] A. Démolis, N. Essayem, F. Rataboul, ACS Sustain. Chem. Eng. 2 (2014) 1338–1352.

[4] K. Yan, G. Wu, T. Lafleur, C. Jarvis, Renew. Sustain. Energy Rev. 38 (2014) 663–676.

[5] E. Ahmad, Md.I. Alam, K.K. Pant, M.A. Haider, Green Chem. 18 (2016) 4804–4823.

[6] Y. Jing, Y. Guo, Q. Xia, X. Liu, Y. Wang, Chem 5 (2019) 2520–2546.

[7] H. Joshi, B.R. Moser, J. Toler, W.F. Smith, T. Walker, Biomass Bioenergy 35 (2011) 3262–3266.

[8] D.R. Jones, S. Iqbal, S. Ishikawa, C. Reece, L.M. Thomas, P.J. Miedziak, D.J. Morgan, J.K. Edwards, J.K. Bartley, D.J. Willock, G.J. Hutchings, Catal. Sci. Technol. 6 (2016) 6022–6030.

[9] X. Liu, H. Pan, H. Zhang, H. Li, S. Yang, ACS Omega 4 (2019) 8390–8399.

[10] Y. Bai, Y. Liu, F. Bai, Q. Sun, L. Li, T. Zhang, Open Chem. 19 (2021) 1294–1300.

[11] T. Chhabra, J. Rohilla, V. Krishnan, Mol. Catal. 519 (2022) 112135.

[12] C. Canon, N. Sanchez, M. Cobo, J. Clean. Prod. 377 (2022) 134276.

[13] Q. Guo, F. Yang, X. Liu, M. Sun, Y. Guo, Y. Wang, Chin. J. Catal. 41 (2020) 1772–1781.

[14] E. Ahmad, K. Kishore Pant, M. Ali Haider, Mater. Sci. Energy Technol. 5 (2022) 189–196.

[15] M. Przypis, K. Matuszek, A. Chrobok, M. Swadźba-Kwaśny, D. Gillner, J. Mol. Liq. 308 (2020) 113166.

[16] S. An, D. Song, B. Lu, X. Yang, Y.-H. Guo, Chem. - Eur. J. 21 (2015) 10786–10798.

[17] W. Zhu, C. Chang, C. Ma, F. Du, Chin. J. Chem. Eng. 22 (2014) 238–242.

[18] P. Demma Carà, R. Ciriminna, N.R. Shiju, G. Rothenberg, M. Pagliaro, ChemSusChem 7 (2014) 835–840.

[19] A. Brzęczek-Szafran, J. Więcławik, N. Barteczko, A. Szelwicka, E. Byrne, A. Kolanowska, M. Swadźba Kwaśny, A. Chrobok, Green Chem. 23 (2021) 4421–4429.

[20] A. Hu, H. Wang, J. Ding, Catal. Lett. 152 (2022) 3158–3167.

[21] G. Zhao, L. Hu, Y. Sun, X. Zeng, L. Lin, BioResources 9 (2014) 2634–2644.

[22] Yogita, B.S. Rao, Ch. Subrahmanyam, N. Lingaiah, New J. Chem. 45 (2021) 3224–3233.

[23] J.-P. Lange, W.D. van de Graaf, R.J. Haan, ChemSusChem 2 (2009) 437–441.

[24] K.Y. Nandiwale, A.M. Pande, V.V. Bokade, RSC Adv. 5 (2015) 79224–79231.

[25] P. Neves, P.A. Russo, A. Fernandes, M.M. Antunes, J. Farinha, M. Pillinger, M.F. Ribeiro, J.E. Castanheiro, A.A. Valente, Appl. Catal. Gen. 487 (2014) 148–157.

[26] R. Prajapati, S. Srivastava, G.C. Jadeja, J. Parikh, Waste Biomass Valorization 14 (2022) 609–618.

[27] X.-F. Liu, H. Li, H. Zhang, H. Pan, S. Huang, K.-L. Yang, S. Yang, RSC Adv. 6 (2016) 90232–90238.

[28] J. Yang, H. Zhang, Z. Ao, S. Zhang, Catal. Commun. 123 (2019) 109–113.

[29] H. Guo, Y. Hirosaki, X. Qi, R. Lee Smith, Renew. Energy 157 (2020) 951–958.

[30] A. Shokrolahi, A. Zali, H.R. Pouretedal, M. Mahdavi, Catal. Commun. 9 (2008) 859–863.

[31] D. Song, S. An, B. Lu, Y. Guo, J. Leng, Appl. Catal. B Environ. 179 (2015) 445–457.

[32] H. Chen, H. Ruan, X. Lu, J. Fu, T. Langrish, X. Lu, Chem. Eng. J. 333 (2018) 434–442.

[33] M. Li, J. Wei, G. Yan, H. Liu, X. Tang, Yong Sun, Xianhai Zeng, Tingzhou Lei, Lu Lin, Renew. Energy 147 (2020) 916–923.

[34] G. Zhao, M. Liu, X. Xia, L. Li, B. Xu, Molecules 24 (2019) 1881.

[35] X. Yu, L. Peng, Q. Pu, R. Tao, X. Gao, L. He, J. Zhang, Res. Chem. Intermed. 46 (2020) 1469–1485.

[36] W. Zhao, P. Salame, V. Herledan, F. Launay, A. Gédéon, T. Qi, J. Porous Mater. 17 (2010) 335–340.

[37] F. Zhou, J. Tang, Z. Fei, X. Zhou, X. Chen, M. Cui, X. Qiao, J. Porous Mater. 21 (2014) 149–155.

[38] K.A. Shah, J.K. Parikh, K.C. Maheria, Catal. Today 237 (2014) 29–37.

[39] S.M.L. dos Santos, K.A.B. Nogueira, M. de Souza Gama, J.D.F. Lima, I.J. da Silva Júnior, D.C.S. de Azevedo, Microporous Mesoporous Mater. 180 (2013) 284–292.

[40] H. Chaudhuri, S. Dash, A. Sarkar, Ind. Eng. Chem. Res. 56 (2017) 2943–2957.

[41] J.A. Janaun, T.J. Mey, A. Bono, D. Krishnaiah, Bull. Chem. React. Eng. Catal. 12 (2017) 41.

[42] M. Niakan, M. Masteri-Farahani, F. Seidi, Fuel 337 (2023) 127242.

[43] G. Wang, Z. Zhang, L. Song, Green Chem 16 (2014) 1436–1443.

[44] E.S. Sankar, K.S. Reddy, Y. Jyothi, B.D. Raju, K.S.R. Rao, Catal. Lett. 147 (2017) 2807–2816.

[45] X.-F. Liu, H. Li, H. Zhang, H. Pan, S. Huang, K.-L. Yang, S. Yang, RSC Adv. 6 (2016) 90232–90238.

[46] Z. Zhang, H. Yuan, Y. Wang, Y. Ke, J. Solid State Chem. 280 (2019) 120991.

[47] X. Li, Y. Li, X. Wang, Q. Peng, W. Hui, ·Aiyun Hu, H. Wang, Catal. Lett. 151 (2021) 2622–2630.

[48] Y. Zhang, X. Wang, T. Hou, H. Liu, L. Han, W. Xiao, J. Energy Chem. 27 (2018) 890–897.

[49] X. Kong, X. Zhang, C. Han, C. Li, L. Yu, J. Liu, Mol. Catal. 443 (2017) 186–192.